The 3rd International Conference on Materials Chemistry and Environmental Engineering
DOI: 10.54254/2755-2721/3/20230537

Mxenes applications in different metal ion batteries

Shukai Hu

Chemistry Department, University College London, London, UK, WC1E 6BT

zccaubx@ucl.ac.uk

Abstract. Mxenes, with unique two-dimensional structures, possess excellent electrical conductivity and low diffusion barriers, which are potential materials used in different metal ion batteries. Herein this paper focuses on synthesising MXenes applications through a literature review method. In relevant analysis, Mxenes can be Constructed in Ultrathin Layered with TiN in Heterostructure to Facilitate the Favorable Catalytic Capability of Lithium–Sulfur Batteries. For Potassium-Ion Batteries, MXene coated in Carbon to form a Three-Dimensional MXene/Iron Selenide Ball with Core–Shell Structure shows a high reversible capacity with significant cycle stability. Ti_3C_2Tx MXene Electrolyte Additive prevents zinc ion batteries from Zinc Dendrite Deposition. Lastly, customizing the MXene nitrogen terminals for Na-Ion Batteries facilitates fast charging and stable cycling even when the temperature is low.

Keywords: lithium-sulfur batteries, potassium-ion batteries, zinc ion batteries, na-ion batteries.

1. Introduction

MXenes are a novel class of substance that was unearthed for the first time in 2011. It has been shown that exfoliating Ti_3AlC2 in HF. at room temperature may produce 2D Ti_3C_2 nanosheets, multilayer structures, and conical scrolls. This finding paves the way for synthesizing many other 2D crystals since Ti_3AlC_2 is a member of a group that contains more than 60 stacked ternary carbides and nitrides [1].

MXenes have the standard chemical formula $M_{n+1}X_nT_x$. They are composed of a transition metal (M) with Carbon or nitrogen atoms (X) and a T that stands for a surface termination, which is most frequently fluorine (F), hydroxyl (OH), or oxygen (O) atoms. The metal and the x are arranged in layers with n values ranging from one to three [2-3]. In Figure 1, atomic diagrams of all three forms of MXenes are shown [4]. With unusual structures, MXenes are distinguished by the unique presence of both a high level of hydrophilicity and metallic conductivity [5]. Since of their one-of-a-kind characteristics, there is a rising interest in these materials, as evidenced by the recently published reviews. MXenes have already been shown to be helpful in various fields, including energy harvesting, osteosarcoma phototherapy, and even water desalination [6-8]. Here we focus on the synthesis MXenes applications which enhance the energy storage performances of different metal ion batteries.

© 2023 The Authors. This is an open access article distributed under the terms of the Creative Commons Attribution License 4.0 (https://creativecommons.org/licenses/by/4.0/).

DOI: 10.54254/2755-2721/3/20230537

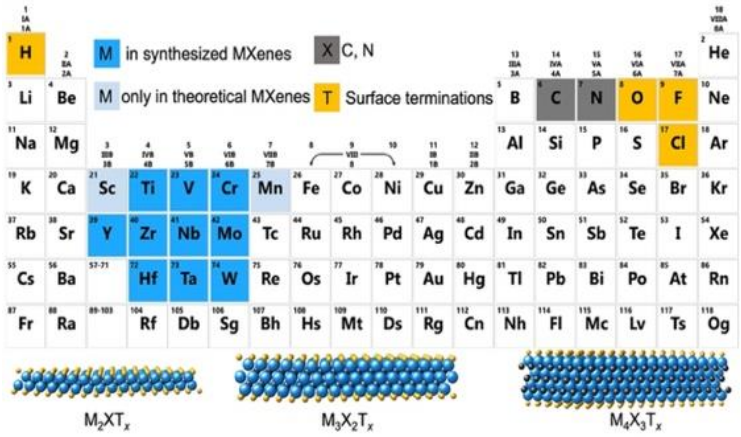

Figure 1. Periodic tables displaying the elements construct MXenes. With schematics of MXenes' three most common structural configurations [4].

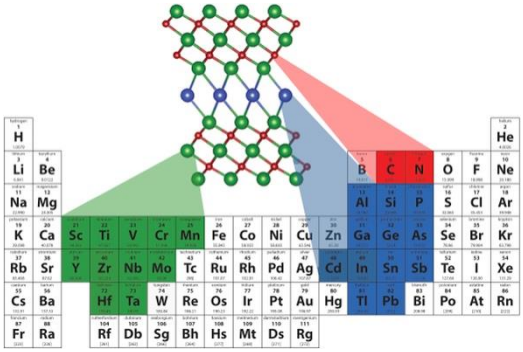

Figure 2. MAX phases $M_{n+1}AX_n$ forming elements [9].

2. MXenes applications

The MAX phase is the starting material for MXenes, which have the formula ($M_{n+1}AXn$) with M and A layers that intercalate in a hexagonal structure and X atoms occupying the M's octahedral positions, where "M" is a d-block transition metal, "A" is an element from groups 13 and 14, and "X" is either carbon or nitrogen, as shown in figure 2 [9]. Due to their low density, high hardness, and corrosion resistance, MXenes are ideal battery foundation materials. Its thermal, electrical, and machinability rival metals [10].

2.1. Application in Lithium–Sulfur Batteries

Soluble intermediate lithium polysulfides induce the shuttle effect in lithium-sulfur batteries (LiPSs) dispersed in liquid electrolytes, the insulating properties of sulfur and Li_2S, and the slow sulfur redox kinetics [11]. Catalysis reduces Li-S batteries' shuttle effect and sluggish reaction kinetics [12]. MXenes can host sulfur [13]. MXene spontaneously restacks to packed film via van der Waals forces and hydrogen bonding. Sulfur loading decreases [14]. Pure MXene lacks chemical immobilization and catalysis [15]. In-situ programmable nitridation builds a hollow spherical structure from ultrathin 2D Ti_3C_2Tx-TiN heterostructures (MX-TiN). With a high-abundance interface area, the 2D heterostructures promote high-density electron flow, boosting electrical conductivity, resistance, and electrochemical reaction kinetics. The TiN (001) surface is more electrically stable, adsorptive, and catalytic. The ultrathin layered heterostructure was regulated to a few nanometers, minimizing electron transport from catalysts to reactive sulfur species and boosting surface area with great adsorptive and catalytic sites. S/MX-TiN cathode offers outstanding long-term cyclability with 0.022% capacity fading over 1000 cycles and 8.27 mAh cm2 areal capacity with high sulfur loading and low electrolytes [16].

DOI: 10.54254/2755-2721/3/20230537

2.2. Application in K-ion batteries

K-ion batteries (KIBS) are becoming attractive for grid energy storage systems due to their high energy density and low cost [17]. The sluggish reaction kinetics and substantial volume expansion caused by K+'s larger diameter than Li+ and Na+ make it challenging to produce electrode materials for high-performance KIBS [18]. This is because K+ has a larger diameter than Li+ and Na+. Mxenes are advantageous electrode materials for alkali-ion batteries because of their solid metallic conductivity and low ion diffusion barrier [19]. MXene nanosheets were used as the starting material to develop a novel synthetic process that converts MXene nanosheets into three-dimensional balls coated with iron selenides and carbon. This process, known as FeSex@C/MB, was designed to prevent MXene nanosheets from readily aggregating and stacking during the drying and electrode fabrication. MXene's two-dimensional structure can be converted into a three-dimensional design to eliminate inefficient restacking between interlayers, enhance the surface area, and transport ions faster while retaining beneficial features. Adding iron selenides and carbon to 3D MXene balls (M.B.s) increases the amount of ion storage sites and strengthens the composite balls. FeSex@C/MB anodes in KIBS have the good reversible capacity, cycle stability, and rate capability [20].

2.3. Application in Zinc metal batteries

Zinc metal batteries have a high theoretical specific capacity (820 mAh g1), low redox potential (0.76 V versus SHE), low cost, large abundance in nature, and good safety [21]. However, Repeated Zn stripping/plating causes permanent dendrite growth [22], which may create internal shorting, reducing cycle life. Moreover, dendrites cause electrochemically inactive by exposing the abnormal surface area of zinc. This issue restricts the Coulombic efficiency [23]. Dendrite-free anodes are needed to improve the performance of rechargeable Zn metal batteries. Ti_3C_2Tx MXene electrolytes improve Zn plating/stripping irreversibility and kinetics. Massive $Zn^{2+}$and MXene additives can form a conductive buffer layer on the Zn electrode by electrostatically combining. MXene- Zn^{2+} can homogenize surface Zn^{2+}. Its well-dispersed "seed patches" may facilitate homogenous nucleation and homogeneous ionic flow during deposition, preventing Zn dendrites. In addition, the presence of MXene sheets in the electrolyte significantly reduces the length of the Zn^{2+} diffusion channels and makes migration of these ions easier; as a result, the plating and striping kinetics will be enhanced. Consequently, the Zn metal anode provides higher cycle stability and high C.E. when utilizing MXene-contained electrolytes. This is the case whether the cell configuration is symmetric or complete [24].

2.4. Application in sodium-ion batteries

According to the Arrhenius formula [25], sodium-ion batteries, also known as SIBs, are promising because of their cheap cost and improved temperature tolerance. Because of this, they will be able to achieve faster charging as well as improved performance from their batteries at lower temperatures. However, their performance at low temperatures is still limited because of the delayed ionic transport in the electrodes that is generated by temperatures below zero, the reduced ion conductivity in the electrolytes, and the increased impedance between the electrode and the electrolyte [26]. This work describes an interlayer-confined technique for designing nitrogen terminals on Ti_3C_2 to decrease the charge transfer barrier and increase the ion's diffusion kinetics. The technique was developed to increase ions diffusion kinetics. Because of this, quick charging can be reached at temperatures lower than 25 degrees Celsius (Scheme 1c). In addition to introducing a nitrogen source into Ti_3C_2 MXene layers to design nitrogen terminals (Ti_3C_2-Nfunct), the presence of pre-intercalated cetyltrimethylammonium bromide (CTAB) also offers support for the layer structure. At the same time, the annealing process is being carried out.

Using X-ray diffraction at varying temperatures in situ, we were able to establish both the structural transition and the production process that corresponded to it (XRD). Customizing the nitrogen terminals would redistribute charge on the Ti3C2 layer, lowering the bandgap, hydrophilicity, and diffusion energy barrier, according to DFT calculations. Comprehensive XPS tests show that the solid electrolyte interface (SEI) formed mainly on Ti_3C_2 and Ti_3C_2-Nfunct electrodes are made of different materials. The

DOI: 10.54254/2755-2721/3/20230537

SEI made on the Ti_3C_2-Nfunct electrode has more inorganic compounds, which are needed for Na+ transfer at the electrode/electrolyte interface. The multi-scale physical caricatures demonstrate that Ti_3C_2-Nfunct may show Na+-solvent co-intercalation, which lets it avoid de-solvation and have fast kinetics at relatively low temperatures. As such, Ti_3C_2-Nfunct anodes at 25 degrees Celsius have a high reversible capacity, charge quickly, and have excellent cycling stability (80.9% after 5000 cycles). Whole cells with $Na_3V_2(PO_{4)2}F_3$ cathodes have a high energy density and capacity retention below 25 degrees Celsius [27].

3. Conclusion

In conclusion, ultrathin 2D Ti_3C_2Tx-TiN heterostructure mxene improved catalytic performance in interfacial areas, sulphur species binding energy for Li–S batteries, carbon-coated 3D MXene/iron selenide balls with aggregation-resistant features, and high-performance KIBS. All of these benefits were achieved through the use of a KIBS. Mxene-containing electrolytes, with their high conductivity and considerable binding energy, prevent the growth of dendrites, and as a result, they uniformly regulate the nucleation of Zinc. Even when the temperature is somewhat low, SIBs can continue to operate at a high-efficiency level thanks to mxenes.

References

[1] Naguib, M. et al. (2011) "Two-dimensional nanocrystals produced by exfoliation of TI3ALC2," Advanced Materials, 23(37), pp. 4248–4253. Available at: https://doi.org/10.1002/adma.201102306.

[2] Verger, L. et al. (2019) "Mxenes: An introduction of their synthesis, select properties, and applications," Trends in Chemistry, 1(7), pp. 656–669. Available at: https://doi.org/10.1016/j.trechm.2019.04.006.

[3] Wei, Y. et al. (2021) "Advances in the synthesis of 2D MXENES," Advanced Materials, 33(39), p. 2103148. Available at: https://doi.org/10.1002/adma.202103148.

[4] Gogotsi, Y. and Anasori, B. (2019) "The rise of Mxenes," ACS Nano, 13(8), pp. 8491–8494. Available at: https://doi.org/10.1021/acsnano.9b06394.

[5] Salim, O. et al. (2019) "Introduction to mxenes: Synthesis and characteristics," Materials Today Chemistry, 14, p. 100191. Available at: https://doi.org/10.1016/j.mtchem.2019.08.010.

[6] Jia, Y. et al. (2021) "Flexible AG microparticle/mxene-based film for Energy Harvesting," Nano-Micro Letters, 13(1). Available at: https://doi.org/10.1007/s40820-021-00729-w.

[7] Lei, Z. et al. (2021) "Nature inspired mxene-decorated 3D honeycomb-fabric architectures toward efficient water desalination and salt harvesting," Nano-Micro Letters, 14(1). Available at: https://doi.org/10.1007/s40820-021-00748-7.

[8] Yin, J. et al. (2021) "NB2C MXene-functionalized scaffolds enable osteosarcoma phototherapy and angiogenesis/osteogenesis of bone defects," Nano-Micro Letters, 13(1). Available at: https://doi.org/10.1007/s40820-020-00547-6.

[9] Ronchi, R.M., Arantes, J.T. and Santos, S.F. (2019) "Synthesis, structure, properties and applications of mxenes: Current status and Perspectives," Ceramics International, 45(15), pp. 18167–18188. Available at: https://doi.org/10.1016/j.ceramint.2019.06.114.

[10] Ronchi, R.M., Arantes, J.T. and Santos, S.F. (2019) "Synthesis, structure, properties and applications of mxenes: Current status and Perspectives," Ceramics International, 45(15), pp. 18167–18188. Available at: https://doi.org/10.1016/j.ceramint.2019.06.114.

[11] Li, C. et al. (2021) "Regulating polysulfide intermediates by Ultrathin Co-Bi nanosheet electrocatalyst in lithium−sulfur batteries," Nano Today, 40, p. 101246. Available at: https://doi.org/10.1016/j.nantod.2021.101246.

[12] Jiang, B. et al. (2021) "High-index faceted nanocrystals as highly efficient bifunctional electrocatalysts for high-performance lithium–sulfur batteries," Nano-Micro Letters, 14(1). Available at: https://doi.org/10.1007/s40820-021-00769-2.

[13] Wang, H. et al. (2022) "Construction of ultrathin layered mxene-tin heterostructure enabling the

favourable catalytic ability for high-areal-capacity lithium–sulfur batteries," Nano-Micro Letters, 14(1). Available at: https://doi.org/10.1007/s40820-022-00935-0.

[14] Bao, W. et al. (2018) "Porous cryo-dried mxene for efficient capacitive deionization," Joule, 2(4), pp. 778–787. Available at: https://doi.org/10.1016/j.joule.2018.02.018.

[15] Jiang, Y. et al. (2019) "Oxygen-functionalized ultrathin ti 3 C 2 T x mxene for enhanced electrocatalytic hydrogen evolution," ChemSusChem, 12(7), pp. 1368–1373. Available at: https://doi.org/10.1002/cssc.201803032.

[16] Wang, H. et al. (2022) "Construction of ultrathin layered mxene-tin heterostructure enabling the favourable catalytic ability for high-areal-capacity lithium–sulfur batteries," Nano-Micro Letters, 14(1). Available at: https://doi.org/10.1007/s40820-022-00935-0.

[17] He, X.-D. et al. (2019) "A three-dimensional macroporous antimony@carbon composite as a high-performance anode material for potassium-ion batteries," Journal of Materials Chemistry A, 7(16), pp. 9629–9637. Available at: https://doi.org/10.1039/c9ta01968e.

[18] Sheng, B. et al. (2020) "Boosting potassium storage by integration advantageous of defect engineering and spatial confinement: A case study of S.B. 2 se 3," Small, 16(49), p. 2005272. Available at: https://doi.org/10.1002/smll.202005272.

[19] Zheng, J. et al. (2020) "Advanced anode materials of potassium ion batteries: From zero dimension to three dimensions," Nano-Micro Letters, 13(1). Available at: https://doi.org/10.1007/s40820-020-00541-y.

[20] Yang, S.H. et al. (2021) "Carbon-coated three-dimensional mxene/iron selenide ball with core–shell structure for high-performance potassium-ion batteries," Nano-Micro Letters, 14(1). Available at: https://doi.org/10.1007/s40820-021-00741-0.

[21] Xu, W. and Wang, Y. (2019) "Recent progress on zinc-ion rechargeable batteries," Nano-Micro Letters, 11(1). Available at: https://doi.org/10.1007/s40820-019-0322-9.

[22] Tang, B. et al. (2019) "Issues and opportunities facing aqueous zinc-ion batteries," Energy & Environmental Science, 12(11), pp. 3288–3304. Available at: https://doi.org/10.1039/c9ee02526j.

[23] Wang, F. et al. (2018) "Highly reversible zinc metal anode for aqueous batteries," Nature Materials, 17(6), pp. 543–549. Available at: https://doi.org/10.1038/s41563-018-0063-z.

[24] Sun, C. et al. (2021) "Interface engineering via ti3c2tx mxene electrolyte additive toward dendrite-free zinc deposition," Nano-Micro Letters, 13(1). Available at: https://doi.org/10.1007/s40820-021-00612-8.

[25] Zhang, W. et al. (2019) "Lowering charge transfer barrier of LIMN2O4 via nickel surface doping to enhance li+ intercalation kinetics at subzero temperatures," Journal of the American Chemical Society, 141(36), pp. 14038–14042. Available at: https://doi.org/10.1021/jacs.9b05531.

[26] He, X.-D. et al. (2019) "A three-dimensional macroporous antimony@carbon composite as a high-performance anode material for potassium-ion batteries," Journal of Materials Chemistry A, 7(16), pp. 9629–9637. Available at: https://doi.org/10.1039/c9ta01968e.

[27] Xia, Y. et al. (2022) "Tailoring nitrogen terminals on mxene enables fast charging and stable cycling Na-ion batteries at low temperature," Nano-Micro Letters, 14(1). Available at: https://doi.org/10.1007/s40820-022-00885-7.